Phantom validation of temperature mapping using fat-water MRI with explicit fitting of water peak location

E. Brian Welch[1,2], Aliya Gifford[2,3], and Theodore F. Towse[2,4]

[1]*Radiology and Radiological Sciences, Vanderbilt University, Nashville, TN, United States,* [2]*Institute of Imaging Science, Vanderbilt University, Nashville, TN, United States,* [3]*Chemical and Physical Biology Program, Vanderbilt University, Nashville, TN, United States,* [4]*Physical Medicine and Rehabilitation, Vanderbilt University, Nashville, TN, United States*

Purpose: The objective of this research was to demonstrate the feasibility of MRI-based thermometry in samples composed of water and fat. This approach should interest MR physicists and clinicians who want to measure temperature in fatty tissue in which the conventional water proton resonance frequency shift method is difficult to apply since lipid protons do not experience a temperature-dependent frequency shift. Besides temperature monitoring of water-containing fatty tissue during interventional applications, this method is well suited for studies of brown adipose tissue (BAT), which is thermogenic and composed of 50-80% fat. A similar method known as water and fat thermal MRI[1] was previously described as detecting relative temperature changes from phase differences between water and fat vectors combined with an average echo time. In this method, frequency shift of the water peak is explicitly modeled. Fitting the water peak location allows absolute thermometry from a single image. In this work the technique was demonstrated using fat-water phantoms undergoing heating and cooling with validation using fiber optic (FO) temperature probes.

Methods: Seven fat-water phantoms with nominal fat fractions of 0, 10, 20, 30, 40, 60 and 100 percent were prepared using peanut oil and agar gel based on a published recipe[2] and imaged using a Philips Achieva 3T (Philips Healthcare, Best, Netherlands) scanner with an 8-channel head coil (Invivo Corp., Gainesville, FL). Ten dynamics of a single-slice, 24-echo multiple fast field echo (mFFE) fat-water MRI sequence were collected with two dynamics at baseline room temperature and eight dynamics after the 0, 20, 40 and 100 percent phantoms were briefly placed in cold water while the 10, 30 and 60 percent phantoms were placed in hot water. Temperatures of the 40% and 60% phantoms were sampled every second using two channels of a FISO Commander 2 (FISO Technologies Inc., Quebec, Canada) FO temperature monitor. Scanner software was modified to acquire 24 echoes acquired as four interleaved sets of six echoes with TE_1=1.5 ms and effective $\Delta TE = 0.625$ ms. Other protocol details included: flip angle = 10º, water fat shift = 0.507 pixels, readout sampling bandwidth = 857.8 Hz/pixel, in-plane field of view = 200 mm × 200 mm, acquired voxel size = 1 mm x 1 mm x 20 mm, TR = 50 ms, dynamic scan time = 40 s. Conventional fat/water separation based on a multi-scale whole-image optimization algorithm[3] was performed for each dynamic. Fat was modeled using 9 peaks[4]. The first echo of each six-echo train was discarded to avoid potential contamination by eddy currents in the complex water-fat signal model. Results of the conventional fat/water separation were used to initialize a modified version of the mixed (magnitude and complex) signal fitting algorithm available in the ISMRM Fat Water Toolbox[5] based on the work[6] of Hernando et al. The mixed signal fitting function was modified to additionally solve for a temperature-dependent frequency shift of the water peak. The equation below captures the employed model for the voxel-by-voxel MR signal $S(t)$ as a function of time t where Δf_T is the off-resonance caused by temperature, W and F are the water and fat magnitudes with complex phase ϕ, α_p and Δf_p are amplitude and frequency of the p^{th} fat spectrum peak, Δf_{B0} is background field off-resonance, and R_2^* is the signal decay rate for both W and F.

$$S(t) = \left(W e^{i 2\pi \Delta f_T t} + F \sum_{p=1}^{P} \alpha_p e^{i 2\pi \Delta f_p t} \right) e^{i\phi} e^{\left(i 2\pi \Delta f_{B0} - R_2^*\right)t}$$

Results: Tables 1 and 2 display the fat signal fraction (FSF) and absolute temperature measurements respectively for each phantom across the 10 dynamics. Measured FSF was consistent except for the entries highlighted in red. Temperatures followed the expected pattern except for those of the 100% fat, 0% fat and entries where the FSF was incorrect. The 100% fat and 0% fat phantoms should not work using this method because they do not contain a mixture of water and lipid protons. Figure 1 shows the relative temperature change measured by FWMRI vs. relative temperature change detected by the FO probes. FWMRI-based measurements followed closely the FO traces except for the points with an FSF error. These results show that explicit modeling of the water peak location in fat-water MRI signal analysis can capture temperature change. Future work is necessary to explore the impact of reducing echoes and of higher artifacts associated with in vivo applications.

References: [1] Soher BJ, et al. MRM 63(5):1238-46; 2010. [2] Hines CDG, et al. JMRI 30(5):1215-22; 2009. [3] Berglund J, et al. MRM 67(6):1684-93; 2012. [4] Hamilton G, et al. NMR Biomed 24:784-790; 2011. [5] Hernando D, et al. ISMRM Fat Water Toolbox v1.0. http://ismrm.org/workshops/FatWater12/data.htm; 2012 [6] Hernando D, et al. MRM 67(3):638-44; 2012.

Acknowledgements: 1R21DK096282 NIDDK/NIH & UL1 TR000445 NCATS/NIH

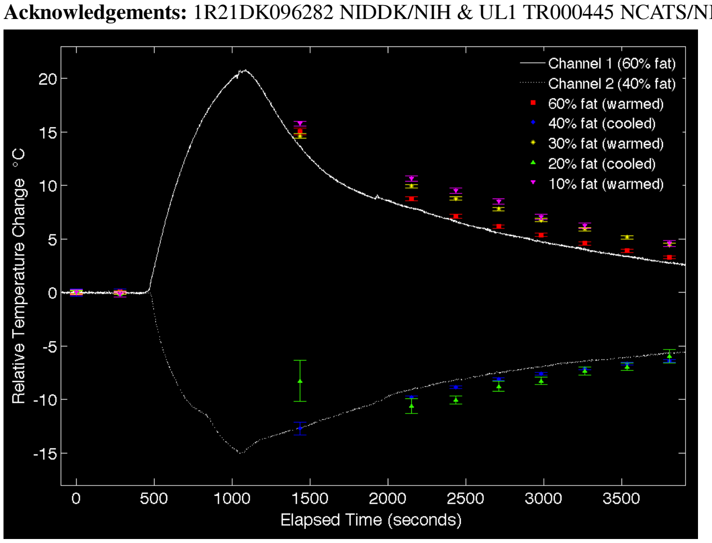

Figure 1. Relative temperature changes detected by fat-water MRI (with water peak location fitting) compared to fiber optic probe measurements.

Table 1. Measured Fat Signal Fractions (mean±95% C.I. half-width)

DYN	100% fat	60% fat	40% fat	30% fat	20% fat	10% fat	0% fat
1	97.75±0.04	59.0±0.1	40.1±0.1	28.8±0.1	18.5±0.1	10.5±0.1	0.9±0.1
2	97.76±0.04	58.9±0.1	40.1±0.1	28.7±0.1	18.5±0.1	10.4±0.1	1.0±0.1
3	96.9±0.6	62.4±0.2	39.0±0.3	32.9±0.1	16.2±0.4	12.9±0.1	1.6±0.1
4	97.3±0.1	61.4±0.1	39.7±0.1	31.4±0.1	17.5±0.2	11.9±0.1	1.0±0.1
5	97.4±0.1	61.1±0.1	39.8±0.1	31.0±0.1	17.6±0.1	11.5±0.1	1.4±0.4
6	97.4±0.1	60.9±0.1	39.9±0.1	30.8±0.1	17.7±0.2	11.4±0.1	1.2±0.3
7	97.4±0.1	60.8±0.1	40.0±0.1	30.6±0.1	17.9±0.1	11.5±0.1	1.3±0.3
8	97.4±0.1	60.6±0.1	40.1±0.1	30.3±0.1	18.0±0.1	11.2±0.1	1.0±0.1
9	97.4±0.1	60.4±0.1	40.0±0.1	30.0±0.1	17.8±0.2	95.92±0.02	1.3±0.3
10	97.3±0.1	60.3±0.1	40.1±0.1	29.9±0.1	17.9±0.2	11.0±0.1	1.0±0.1

Table 2. Measured Absolute Temperature in °C (mean±95% C.I. half-width)

DYN	100% fat	60% fat	40% fat	30% fat	20% fat	10% fat	0% fat
1	10.9±1.0	24.3±0.1	26.8±0.4	24.4±0.2	24.0±0.2	24.4±0.3	33.9±1.6
2	11.0±1.0	24.4±0.1	26.8±0.4	24.3±0.2	23.9±0.2	24.3±0.3	35.9±1.8
3	19.5±2.2	39.4±0.3	14.1±0.6	39.0±0.2	15.8±1.9	40.2±0.2	42.2±1.9
4	19.8±2.2	33.1±0.2	17.0±0.1	34.3±0.2	13.4±0.7	35.1±0.2	41.3±1.5
5	20.2±2.3	31.4±0.2	18.0±0.1	33.1±0.2	14.0±0.4	33.9±0.2	42.2±1.6
6	19.1±2.1	30.5±0.2	18.7±0.1	32.2±0.2	15.3±0.5	32.9±0.2	42.8±1.6
7	18.6±2.2	29.7±0.1	19.3±0.1	31.1±0.1	15.8±0.4	31.5±0.3	40.0±1.7
8	18.8±2.3	28.9±0.1	19.7±0.1	30.3±0.2	16.7±0.4	30.7±0.3	39.7±1.9
9	17.6±1.9	28.2±0.1	20.2±0.1	29.5±0.2	17.1±0.4	40.8±0.3	41.9±1.8
10	18.4±2.1	27.6±0.1	20.4±0.1	28.8±0.2	18.1±0.6	29.0±0.3	38.6±1.9